

Article

Multi-Objective Optimization of Gateway Location Selection in Long-Range Wide Area Networks: A Tradeoff Analysis between System Costs and Bitrate Maximization

Charuay Savithi ¹ and Chutchai Kaewta ^{2,*} 

¹ Smart City Management and Digital Innovation, Mahasarakham Business School, Mahasarakham University, Kantharawichai, Mahasarakham 44150, Thailand; charuay.s@msu.ac.th

² Digital Innovation, Faculty of Computer Science, Ubon Ratchathani Rajabhat University, Mueang, Ubon Ratchathani 34000, Thailand

* Correspondence: chutchai.k@ubru.ac.th

Abstract: LoRaWANs play a critical role in various applications such as smart farming, industrial IoT, and smart cities. The strategic placement of gateways significantly influences network performance optimization. This study presents a comprehensive analysis of the tradeoffs between system costs and bitrate maximization for selecting optimal gateway locations in LoRaWANs. To address this challenge, a rigorous mathematical model is formulated to incorporate essential factors and constraints related to gateway selection. Furthermore, we propose an innovative metaheuristic algorithm known as the M-VaNSAS algorithm, which effectively explores the solution space and identifies favorable gateway locations. The Pareto front and TOPSIS methods are employed to evaluate and rank the generated solutions, providing a robust assessment framework. Our research findings highlight the suitability of a network model comprising 144 gateways tailored for the Ubon Ratchathani province. Among the evaluated algorithms, the M-VaNSAS method demonstrates exceptional efficiency in gateway location selection, outperforming the PSO, DE, and GA methods.

Keywords: gateway location selection; LoRaWANs; multi-objective optimization; system costs; metaheuristic algorithm



Citation: Savithi, C.; Kaewta, C. Multi-Objective Optimization of Gateway Location Selection in Long-Range Wide Area Networks: A Tradeoff Analysis between System Costs and Bitrate Maximization. *J. Sens. Actuator Netw.* **2024**, *13*, 3. <https://doi.org/10.3390/jsan13010003>

Academic Editor: Lei Shu

Received: 29 November 2023

Revised: 27 December 2023

Accepted: 29 December 2023

Published: 2 January 2024



Copyright: © 2024 by the authors. Licensee MDPI, Basel, Switzerland. This article is an open access article distributed under the terms and conditions of the Creative Commons Attribution (CC BY) license (<https://creativecommons.org/licenses/by/4.0/>).

1. Introduction

The 2022 Global Report on Food Crises (GRFC 2022) has shed light on the alarming global food crisis, impacting approximately 193 million individuals in 53 countries, leading to severe food insecurity [1]. This crisis has emerged due to a combination of factors, including geopolitical conflicts, the COVID-19 pandemic, rising food and fuel prices, and rapid population growth. As a result, the agricultural sector is compelled to embrace innovative approaches to meet the escalating demand for food production. Among these approaches, smart farming has garnered significant attention for its potential to revolutionize traditional agricultural practices into highly efficient and technologically advanced systems [2].

Smart farming integrates advanced technologies including big data analytics, cloud computing infrastructure, image processing techniques, machine learning algorithms, and wireless sensor networks [3]. These technologies enable real-time data acquisition, streamline labor-intensive operations, and optimize agricultural production in terms of quality and quantity [4]. The Internet of Things (IoT) plays a crucial role in driving the advancement of smart farming, and finding practical utility in various domains including agriculture, smart cities, and healthcare [5–7]. However, the deployment of smart farming in the rural areas of Thailand poses significant challenges due to limited network infrastructure. Rural agricultural regions are often located far from urban centers, making traditional network infrastructure investment economically infeasible. While cellular networks can provide

signal distribution through Wi-Fi routers, their coverage range is limited to approximately 100 m, rendering them inadequate for large agricultural areas [8].

LPWAN technology has emerged as a critical enabler for empowering smart farming applications by facilitating seamless connectivity between IoT devices and cloud computing systems, enabling efficient data processing [9,10]. LPWAN technology exhibits the ability to transmit signals to both urban and rural areas, covering distances of 5 km in urban environments and 15 km in rural regions [11]. LPWAN technologies, designed to meet the growing demand for IoT devices, have garnered significant attention from academia and industry, offering broad area connectivity, optimized data rates, power consumption, and throughput on licensed and unlicensed frequency bands [7,12,13].

A comprehensive comparative analysis [13,14] examined different LPWAN technologies, highlighting the exceptional capabilities of LoRa technology for large-scale IoT deployments. Moreover, the authors of [15] conducted an extensive investigation, assessing the performance of wireless sensor network systems, emphasizing the remarkable efficiency achieved through the utilization of LoRa–Zigbee hybrid communication. The research provides substantial evidence supporting the superior outcomes derived from the synergistic implementation of these technologies. Consequently, LoRaWAN technology has emerged as the leading communication network within the LPWAN domain for IoT applications in smart agriculture, particularly in rural environments [8,16].

The precise placement of LoRaWAN gateways plays a pivotal role in influencing critical factors such as cost, gateway capacity, bitrate, and quality of service, thereby ensuring the efficient and reliable operation of the network. Extensive research has emphasized the substantial benefits derived from optimizing gateway placement, including a potential 40% reduction in the required number of gateways and a 70% decrease in collision probability [17]. In vast agricultural regions, the utilization of clustering algorithms such as k-means and fuzzy c-means enhances uplink delivery rates and diminishes energy consumption [18]. Furthermore, the particle swarm optimization (PSO) approach effectively identifies optimal gateway locations, yielding superior outcomes with an increasing number of gateways [19]. The placement of gateways significantly influences the energy consumption of end devices, a critical factor for preserving battery life and autonomy [20]. The meticulous identification of optimal gateway locations is crucial for ensuring comprehensive coverage [21,22]. In the study “LoRa-Based IoT Network Assessment in Rural and Urban Scenarios” [23], the authors evaluated the performance of LoRa networks in diverse environments, emphasizing the importance of optimizing parameters for successful smart network deployment. Additionally, a study on gateway positioning strategies in a LoRaWAN [24], compared various algorithms and grid-based methods, recommending fuzzy c-means and Gustafson–Kessel algorithms for enhanced performance and cost-effectiveness in gateway placement.

In this comprehensive examination, we delineate the gateway location selection problem within the framework of a LoRaWAN, encompassing considerations of cost, gateway capacity, and bitrate. Figure 1 depicts the relationship between the gateway and the village, addressing crucial factors such as the foundational costs of establishing a gateway station, station setup expenditures, and gateway capacity. The village comprises end nodes poised to receive signals from the gateway, with the distance between these nodes facilitating signal reception. A strategic emphasis on cost considerations results in the meticulous allocation of a limited number of gateways, leading to reduced costs and a corresponding decrease in average bitrate. Conversely, prioritizing bitrate optimization entails the allocation of a more extensive gateway coverage to achieve equitable signal distribution, consequently incurring higher costs. The intricate interplay between system cost and bitrate maximization constitutes the central focus of our research exploration.

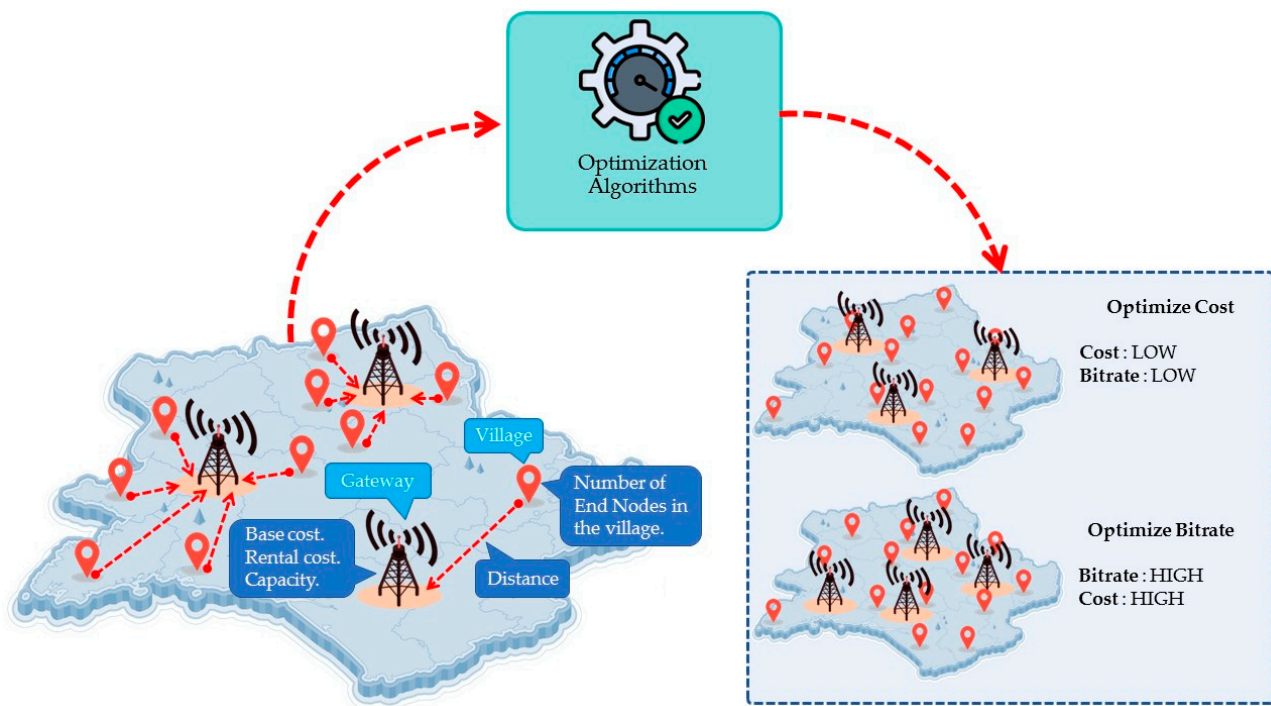


Figure 1. Gateway location selection problem in LoRaWANs.

To evaluate the proposed algorithm’s effectiveness, a real case study conducted in the Ubon Ratchathani province of Thailand is presented. This study focuses on the multiple gateway location selection problem in LoRaWANs and utilizes data on village information, including location, distance, and the number of farms or agricultural households requiring LoRa signal coverage, as well as information on LoRaWAN gateway properties such as base cost, variable cost, capacity, range, and bitrate. The primary objectives of this research are twofold (1) to optimize the total system costs, with an emphasis on cost minimization, and (2) to maximize the bitrate for achieving comprehensive signal coverage across the network. To fulfill the desired goals, a multi-objective gateway location selection model is created, and the effectiveness of the objective function is assessed using Pareto front analysis and the weighted sum approach in conjunction with the TOPSIS method. The key contributions of this study are as follows:

1. Development of multiple gateway location selection models to optimize total system costs and maximize bitrate for efficient signal coverage;
2. Introduction of the novel M-VaNSAS algorithm, specifically tailored for solving the multiple gateway location selection problem in LoRaWANs;
3. Comparative analysis of the M-VaNSAS algorithm against other popular optimization algorithms such as the genetic algorithm (GA), differential evolution algorithm (DE), and particle swarm optimization algorithm (PSO).

The paper is organized as follows. Section 2, Related Works, offers a thorough review of studies concerning gateway location selection in long-range wide area networks. Section 3 provides a comprehensive overview of LoRa and LoRaWAN. In Section 4, we present the methodology, which includes data collection, the development of the mathematical model problem formulation, and our proposed method. Section 5 presents the computational results and framework. Finally, Section 6 presents a comprehensive summary and offers valuable perspectives on prospective areas for further investigation.

2. Related Works

LoRaWANs are integral components of IoT infrastructures, connecting devices over extensive geographical areas. Effective gateway placement is paramount for achieving

comprehensive coverage, efficient communication, and ensuring the overall success of IoT applications. This paper reviews the existing literature, emphasizing the multi-objective optimization of gateway location selection in LoRaWANs, specifically addressing the trade-off between system costs and bitrate maximization.

The gateway placement problem in LoRaWANs is multifaceted, involving considerations such as coverage, spectral efficiency, network redundancy, and system costs. Research by [21] underscored the importance of achieving complete coverage while respecting constraints such as the number of nodes served per access point and required redundancy. Their *k*-dominating set concept introduced a greedy algorithm, demonstrating efficacy in both randomly generated and real smart metering network topologies. In a complementary approach, the authors of [22] developed a mathematical model for optimizing coverage, utilizing the LINGO modeling program. The spatial distribution of clients, radio signal propagation, gateway capacity, topography, obstacles, and network redundancy were identified as pivotal factors influencing gateway placement decisions. This holistic model provides insights into the intricate interplay of these factors, offering a comprehensive approach to gateway location selection.

Dynamic IoT applications were addressed in [25], where the DPLACE model integrates operational and capital expenses (OPEX and CAPEX) with quality of service (QoS) requirements. Leveraging *k*-means and fuzzy *c*-means algorithms, DPLACE optimizes gateway placement, emphasizing the dynamic nature of IoT deployments. Similarly, authors of [26] focused on low-power wide-area sensor networks, proposing greedy algorithms for optimal gateway locations with a focus on interference cancellation and power considerations. To balance costs and efficiency in large-scale IoT applications, the authors of [27] introduced an integer linear programming (ILP) approach. This research underscored the critical role of gateway placement decisions in minimizing network costs while meeting QoS requirements.

A study by [28] explored the impact of gateway placement on network performance, introducing a discounted upper confidence bound (DUCB) multi-armed bandit (MAB) algorithm. The algorithm optimizes LoRa parameters, showcasing improvements in energy efficiency and overall performance. Scalability concerns were addressed in [29], evaluating the potential of LoRa networks through dynamic communication parameter selection and the introduction of multiple sinks. Strategic implementation strategies were emphasized to overcome capacity limitations and ensure scalability. In the context of specific applications, the authors of [30] evaluated the feasibility of LoRaWAN technology for coordinating interface protection systems in smart grids. Their study provides insights into the number of devices a single gateway can manage and corresponding response times, highlighting the adaptability of LoRaWAN technology. The authors of [31] focused on optimizing gateway placement in low-height networks, such as smart irrigation systems. The proposed dynamic programming algorithm aimed to improve the efficiency and reliability of LoRa communication in real-world scenarios. Enhancements and optimizations for LoRaWANs were proposed in [32], introducing the duty cycle gateway selection (DCGS) algorithm. DCGS distributes downlink traffic among available gateways based on their duty cycle time off, improving confirmed packet delivery rates and reducing retransmissions and collisions.

The ReLoRaWAN framework, presented in [33], collaborates with multiple gateways to recover distorted packet payloads. The tri-operation integrated data recovery (TIDR) algorithm significantly improves packet delivery ratio and end device power consumption compared to existing works. In conclusion, this literature review underscores the complexity of gateway placement in LoRaWANs, emphasizing the need to consider factors such as coverage, cost, interference, and application-specific requirements. The methodologies proposed in the reviewed studies provide valuable insights into addressing the gateway placement problem, contributing to the overall efficiency and reliability of LoRaWANs. Tradeoff analysis between system costs and bitrate maximization is a critical aspect of this optimization process, requiring careful consideration of various factors to ensure the seamless integration of IoT applications over extensive geographical areas. The diverse

studies presented collectively contribute to a comprehensive understanding of gateway placement in LoRaWANs, offering insights into optimizing coverage, minimizing costs, and enhancing overall network performance. A summarized overview of the related work is shown in Table 1.

Table 1. Comparison of research contributions.

Study	Factors Considered	Optimization Methods	Main Contributions
[21]	Coverage, redundancy	Greedy algorithm	K-dominating set concept for gateway selection, and evaluation on smart metering networks.
[22]	Coverage, topography, Redundancy	Mathematical model	The LINGO modeling program is used to optimize coverage, considering spatial distribution and obstacles.
[23]	OPEX, CAPEX, QoS	K-means, fuzzy c-means	DPLACE model for dynamic IoT applications, balancing operational and capital expenses.
[24]	Interference, power	Greedy algorithms	Optimizing gateway locations in low-power wide-area sensor networks with a focus on interference cancellation.
[25]	Cost, QoS	Integer linear programming	ILP approach for minimizing network cost with respect to device deployment, and meeting QoS requirements.
[26]	LoRa parameter optimization	Discounted upper confidence Bound MAB	DUCB MAB algorithm to optimize LoRa parameters, and improve energy efficiency, and overall performance.
[28]	System capacity, response time	Feasibility evaluation	Evaluation of LoRaWAN technology for coordinating interface protection systems in smart grids.
[29]	Efficiency, reliability	Dynamic programming algorithm	Optimization of gateway placement in low-height networks, focusing on smart irrigation systems.
[30]	Downlink traffic, reliability	Duty cycle gateway selection	DCGS algorithm for improved downlink traffic distribution among gateways, reducing retransmissions and collisions.
[31]	Packet payload recovery, QoS	Tri-operation integrated data recovery	ReLoRaWAN framework with TIDR algorithm for enhanced packet delivery ratio and reduced end device power consumption.
[27]	Scalability, interference	Dynamic communication parameters	Evaluation of LoRa network scalability, suggesting dynamic communication parameter selection and multiple sinks.
This work	System costs, bitrate Maximization	M-VaNSAS	Trade-off analysis between system costs and bitrate maximization in gateway location selection for LoRaWANs.

Table 1 presents a comparison in which the current study explores a multi-objective optimization problem, emphasizing a trade-off analysis between system costs and the maximization of bitrate in the selection of LoRaWAN gateway locations. This research adds to existing knowledge by offering insights into the complexities of optimizing coverage, reducing costs, and maximizing bitrate within the framework of large-scale IoT deployments. This study's distinctive perspective and methodology contribute to the continuous conversation on effective gateway placement, thereby improving the reliability and efficiency of LoRaWANs.

3. LoRa and LoRaWAN Overview

LoRa (long-range) technology has emerged as an innovative solution that revolutionizes smart cities across multiple domains such as smart environment, smart mobility, smart energy, and smart living. Developed specifically for low-power wide area networks (LPWANs), LoRa utilizes chirp spread spectrum (CSS), a highly effective spread spectrum modulation technique. This enables LoRa to provide reliable, long-range wireless communication, with impressive coverage of up to 5 km in urban environments and 15 km in rural regions [11]. In Thailand, LoRa implementations adhere to the AS923 MHz standard for unlicensed bands, and the adoption of the 920–925 MHz frequency band has been observed [34]. The fundamental parameters in LoRa modulation consist of the spreading factor (SF), bandwidth (BW), and code rate (CR). LoRa modulation supports six spreading factors ranging from SF7 to SF12, each associated with a specific bit rate and estimated range, as detailed in Table 2 [11,35].

Table 2. Comparison of the six different spreading factors.

Spreading Factor	Bitrate	Time on Air	Range
SF7	5470 bit/s	56 ms	2 km
SF8	3125 bit/s	100 ms	4 km
SF9	1760 bit/s	200 ms	6 km
SF10	980 bit/s	370 ms	8 km
SF11	440 bit/s	740 ms	11 km
SF12	290 bit/s	1400 ms	14 km

Table 2 provides a comprehensive comparison of the six spreading factors (SF7 to SF12), presenting their respective bit-rates, time on air (ToA) for uplink messages on a 125 kHz bandwidth, coding rate (CR) 4/5, packet error rate (PER) of 1%, and estimated ranges in rural environments. The duration of airtime values corresponds to a payload size of 10 bytes for each spreading factor. Decreasing the spreading factors leads to increased bit rates, decreased time on air, and reduced transmission ranges. Conversely, increasing the spreading factors results in decreased bit rates, longer time on air, and extended transmission ranges. LoRaWANs (long-range wide area networks), established under the guidance of the LoRa Alliance, a renowned non-profit organization shaping global communication standards, leverage the benefits of LoRa technology. These advantages encompass reduced noise, mitigated interference, and amplified channel capacity. These networks facilitate the expansion of wide-area networks by seamlessly connecting end nodes to cloud computing platforms through LoRaWAN gateways. In LoRaWANs, gateways play a crucial role as intermediaries, efficiently enabling the exchange of information between end devices and a central core network server. It is noteworthy that LoRaWANs exhibit remarkable efficiency when it comes to transmitting small data packets, particularly those containing sensor readings [36]. Figure 2 depicts the architectural framework of LoRaWANs.

Figure 2 presents an illustrative representation of the key components that constitute the foundational framework of the LoRaWAN system. These essential components encompass end nodes, gateways, network servers, and an application server. End nodes serve a vital role in the system, as they are responsible for transmitting sensor data and receiving commands from the network server, enabling access to information and control over devices. Within the LoRaWAN protocol, there are three distinct classes of end nodes Class A, B, and C. Gateways act as intermediaries in the system architecture, intercepting LoRa signals transmitted by end nodes and relaying the data to the server through internet protocol (IP). This enables seamless and uninterrupted communication between the end nodes and the network server. The network servers play a crucial role in the system’s operation by handling the processing of data received from gateways. They perform tasks such as data management, security enforcement, and routing optimization. Application servers or applications utilize the data obtained from the network server to enable various

functionalities and services. They leverage the processed data to derive insights, trigger actions, and provide valuable applications for end-users.

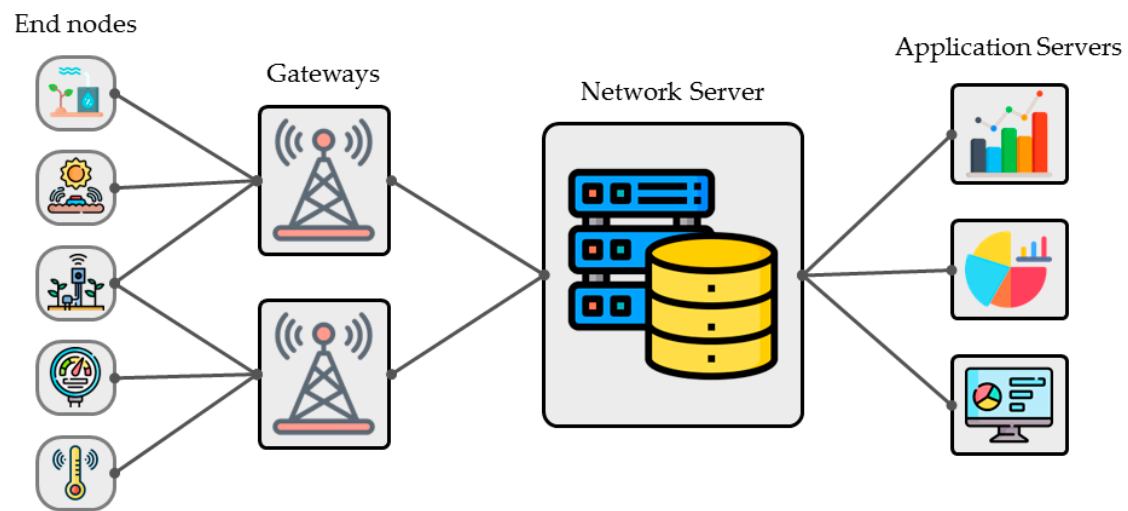


Figure 2. The architectural framework of LoRaWANs.

4. Methodology

In our research methodology, we aim to achieve the optimal selection of gateway locations in LoRaWANs by analyzing the tradeoffs between system costs and bitrate maximization. Our approach considers the distinctive attributes and deployment limitations of the network, ensuring a comprehensive and customized methodology for gateway selection. This section encompasses three key components: data collection, mathematical model formulation, and the proposed method.

Figure 3 illustrates a comprehensive framework for the optimal selection of gateway locations in LoRaWANs. In the data collection phase, critical parameters such as the number of end nodes, villages, base cost, rental cost, capacity, and bitrate scores across different range categories were gathered from reputable agencies. The gateway location selection problem section introduces a mathematical model addressing the optimal selection of gateway locations, offering a detailed problem statement and a systematic approach. The optimization section introduces the M-VaNSAS algorithm, employing a four-step process for effective solution identification. Implementing multi-objective optimization methods focuses on the Pareto front and TOPSIS, utilizing them to manage conflicting objectives. The best solution, derived from M-VaNSAS analysis, undergoes meticulous evaluation to optimize system costs and maximize bitrate, contributing to the overarching goal of achieving the most suitable gateway location selection in LoRaWANs while considering tradeoffs between system costs and bitrate maximization.

4.1. Data Collection

To achieve our objectives, we gathered secondary data from reputable agencies, concentrating on critical parameters such as the number of end nodes, villages, base cost, rental cost, capacity, and bitrate scores across different range categories. These data played a critical role in establishing our methodology. The data collection process involved compiling information based on the parameters and values presented in Tables 3 and 4.

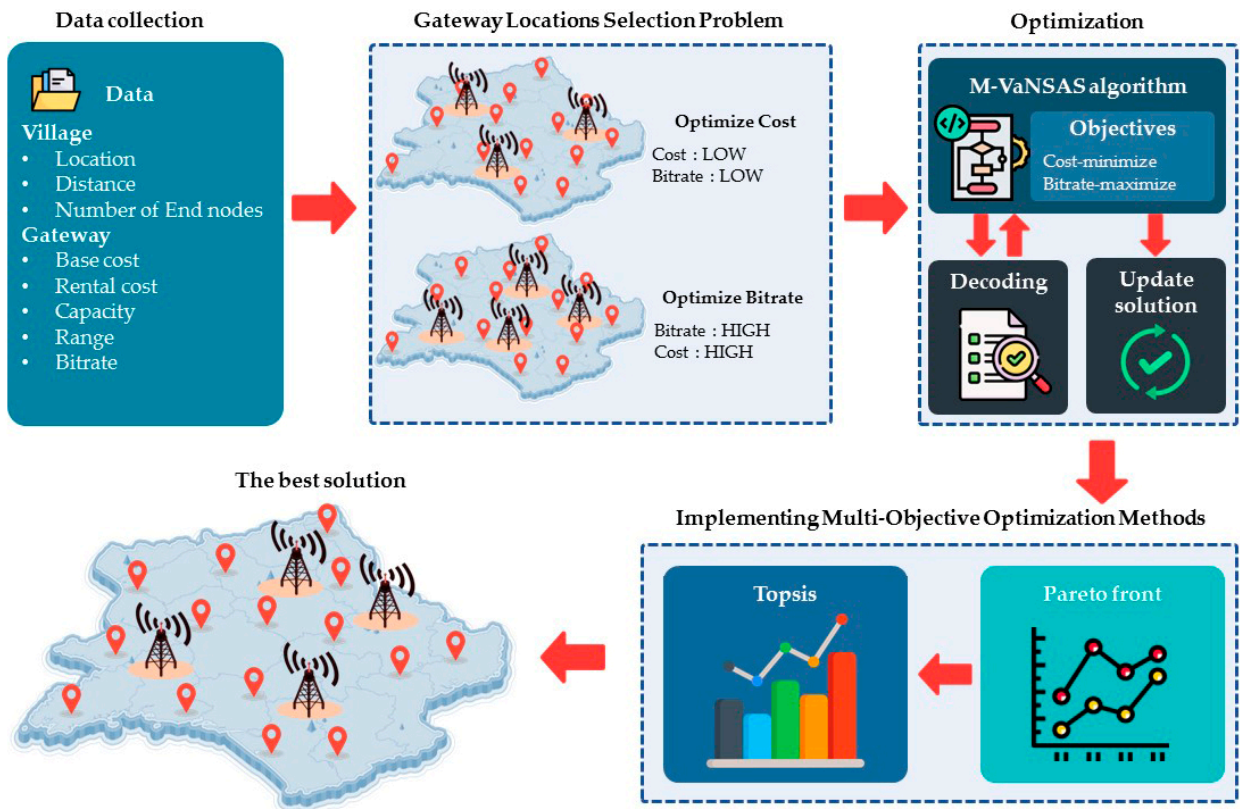


Figure 3. The framework of an optimal selection of gateway locations in LoRaWANs.

Table 3. Parameters and corresponding values.

Parameter	Value
End nodes	295,942
Villages	2199
Base cost (THB)	100,000
Rental cost (THB)	5000–30,000
Capacity (capacity per gateway)	2500
Location	The actual village location from the case study
Distance	Calculated distance using the Haversine formula [37]

Table 4. Evaluation of the bitrate scores.

Range	Bitrate Scores
0–2 km	4
3–4 km	3
5–6 km	2
7–8 km	1

Table 3 outlines the key parameters and their corresponding values. The dataset comprises 295,942 end nodes distributed across 2199 villages within the Ubon Ratchathani province. The initial cost associated with the establishment of a LoRaWAN gateway station is fixed at THB 100,000 per gateway. This serves as the base investment required to set up a functional LoRaWAN gateway, while the rental cost varies from THB 5000 to 30,000, exhibiting random fluctuations within this range. Furthermore, the capacity parameter signifies the capability of a LoRaWAN gateway service to support 2500 end nodes per gateway.

Table 4 presents an assessment of the bitrate scores allocated to various distance categories between the LoRaWAN gateway and the corresponding villages (B_{rv} —the bitrate

performance score for the distance between location r and village v). This evaluation provides insights into the performance of data transmission rates across different ranges in the LoRaWAN infrastructure. These scores assume a critical role in assessing the communication quality between the gateway and the end nodes at varying distances. The scoring system assigns a bitrate score of 4 to range distances of 0–2 km, indicating the highest level of data transmission efficiency. As the range extends to 3–4 km, the score diminishes to 3, signifying a slight reduction in performance. For distances of 5–6 km, the bitrate score further decreases to 2, indicating a decline in transmission capacity. Finally, distances spanning 7–8 km receive the lowest bitrate score of 1, indicating the most limited data transmission capability.

4.2. Gateway Location Selection Problem

To achieve an optimal selection of gateway locations in LoRaWANs, it is crucial to account for both the system costs and the quality of service. This section provides a comprehensive problem statement and presents a mathematical model for the optimal selection of multiple gateway locations in LoRaWANs, considering the aforementioned factors.

Indices

- r, l The location of LoRaWAN gateways, where $r, l = 1 \dots R$;
- v The villages under consideration, where $v = 1 \dots V$.

Parameters

- R The total number of permissible locations for deploying LoRaWAN gateways, R ;
- V The overall count of villages, V ;
- T^1 The maximum signal range of coverage between a LoRaWAN gateway and a village;
- P_v The count of populations accessing a LoRaWAN gateway within village v ;
- D_{rv} The distance separating location r and village v ;
- B_{rv} The bitrate performance score for the distance between location r and village v ;
- C_r The operational capacity of LoRaWAN gateway r ;
- U_r The cost of leasing the space for the station location of LoRaWAN gateway r .

Decision Variables

$$Y_r = \begin{cases} 1 & \text{if location } r \text{ is used to locate the LoRaWAN} \\ 0 & \text{otherwise} \end{cases}$$

$$X_{rv} = \begin{cases} 1 & \text{if location } r \text{ serve village } v \text{ and the distance of } r \text{ and } v \text{ higher than } T^1 \\ 0 & \text{otherwise} \end{cases}$$

Objective Functions

$$\text{Min } Z1 = \sum_{r=1}^R U_r Y_r \tag{1}$$

$$\text{Max } Z2 = \sum_{v=1}^V \sum_{r=1}^R X_{rv} B_{rv} \tag{2}$$

Subject To

$$\sum_{r=1}^R X_{rv} \geq 1 \quad \forall v = 1 \dots V \tag{3}$$

$$X_{rv} \leq Y_r \quad \forall v = 1 \dots V, r = 1 \dots R \tag{4}$$

$$X_{rv} D_{rv} \leq T^1 \quad \forall v = 1 \dots V, r = 1 \dots R \tag{5}$$

$$\sum_{v=1}^V X_{rv} P_v \leq C_r \quad \forall r = 1 \dots R \tag{6}$$

$$X_{rv}, Y_r \in \{0, 1\} \quad \forall v = 1 \dots V, r = 1 \dots R \tag{7}$$

Equation (1) represents the primary objective function, designed to optimize the overall cost incurred during the deployment of LoRaWAN gateways. In contrast, Equation (2) corresponds to the secondary objective function, targeting bitrate perfor-

mance maximization. Equation (3) encompasses the constraints that guarantee each village is adequately served by at least one LoRaWAN gateway. Moreover, Equation (4) introduces constraints that restrict a LoRaWAN gateway positioned at location r to only serve village v if it is deployed at that specific location. To ensure adherence to the defined coverage range, Equation (5) imposes limitations on the distance between LoRaWAN gateway r and village v , ensuring it remains within the permissible maximum distance. Furthermore, Equation (6) enforces constraints on the total number of end nodes served by gateway r to align with its designated capacity. Lastly, Equation (7) defines constraints that stipulate the binary nature of decision variables X_{rv} and $Y_{r,r}$, which signify the selection of gateway locations. The mathematical model formulated in this study considers both cost optimization and bitrate maximization while adhering to constraints that ensure efficient and reliable LoRaWAN operation.

4.3. Optimization

In this research, we introduce a novel metaheuristic algorithm called the M-VaNSAS algorithm. This algorithm has been meticulously designed to effectively navigate diverse solution spaces and identify the most optimal solutions [38]. The M-VaNSAS algorithm follows a structured four-step approach: (1) generating an initial population of trajectories known as tracks, (2) conducting an extensive exploration of routes using black box operators, (3) continuously updating heuristic information by adapting the tracks, and (4) iterative refinement through repeated execution of steps (2) and (3) until the specified termination conditions are satisfied [39]. In the subsequent sections, we provide a comprehensive explanation of our implementation of the M-VaNSAS algorithm to tackle the problem under investigation.

4.3.1. Initial Population Generation

To commence, an initial population of tracks (PT) is created by randomly generating a specified number of tracks. As an illustration, Table 5 presents an example with five tracks; each vector within the set possesses a dimension of $1 \times D$, where D denotes the total number of villages. In this study, D is set to 10. The initial tracks are generated by uniformly selecting real numbers between 0 and 1, utilizing Equation (8):

$$X_{ij1} = U(0, 1) \tag{8}$$

where X_{ij1} represents the value at position j in track i during the first iteration. The index j represents the number of villages, while i corresponds to the predefined number of tracks. Moreover, the algorithm generates two distinct sets of tracks, namely the optimal tracks (BT) set and the random tracks (RT) set. In the first iteration, the BT set is formed by collecting the best solution discovered in iterations 1 through t , and the RT set is randomly chosen, using Equations (9) and (10), respectively.

$$B_{ij1} = U(0, 1) \tag{9}$$

$$R_{ij1} = U(0, 1) \tag{10}$$

Table 5. Initial track configurations.

Villages	1	2	3	4	5	6	7	8	9	10
Track 1	0.74	0.20	0.73	0.84	0.12	0.32	0.09	0.29	0.27	0.82
Track 2	0.12	0.52	0.64	0.88	0.91	0.13	0.62	0.70	0.83	0.29
Track 3	0.66	0.79	0.64	0.07	0.08	0.90	0.94	0.23	0.10	1.00
Track 4	0.86	0.37	0.31	0.99	0.87	0.97	0.61	0.11	0.28	0.48
Track 5	0.10	0.07	0.42	0.79	0.10	0.61	0.92	0.68	0.77	0.61

In Equations (9) and (10), B_{ijt} represents the set of best solutions collected from iterations 1 through t , while R_{ijt} is selected randomly according to the provided formula.

The values of R_{ijt} are updated using Equation (11), where the value of R_{ij} in iteration $t + 1$ is equal to the value of R_{ij} in iteration t , utilizing a chosen IB operator. An exemplary demonstration of five tracks, randomly generated, can be observed in Table 5.

Table 5 presents an illustrative example consisting of five randomly generated tracks. For instance, Track 1 consists of ten villages with corresponding values of 0.74, 0.20, 0.73, 0.84, 0.12, 0.32, 0.09, 0.29, 0.27, and 0.82. These values represent the contributions of the villages to the problem solution and are further decoded using the decoding method.

The decoding procedure employed in this study encompasses three sequential steps. Firstly, the villages are allocated to available LoRaWAN gateways while ensuring that each village is served by at least one gateway and that the maximum distance and total population constraints of each gateway are not violated. Secondly, the element values are sorted in ascending order. Lastly, the assigned LoRaWAN gateways are positioned at the initial slots, and the remaining villages are subsequently assigned to the remaining gateways. This iterative process continues until a viable solution is achieved during the assignment phase. The detailed steps of the decoding method are elaborated as follows:

Table 6 exhibits the sorting outcomes of the element values in Track 1. Initially, the values for Villages 1 to 10 are 0.74, 0.20, 0.73, 0.84, 0.12, 0.32, 0.09, 0.29, 0.27, and 0.82, respectively. These values are arranged in ascending order based on their magnitudes, resulting in the new sequence of villages: 7, 5, 2, 9, 8, 6, 3, 1, 10, and 4. The corresponding values are 0.09, 0.12, 0.20, 0.27, 0.29, 0.32, 0.73, 0.74, 0.82, and 0.84. This sorted sequence is subsequently employed in the subsequent steps of the proposed decoding method.

Table 6. Sorting results of village element values (Track 1).

Before sort	Villages	1	2	3	4	5	6	7	8	9	10
	Value	0.74	0.20	0.73	0.84	0.12	0.32	0.09	0.29	0.27	0.82
After sort	Villages	7	5	2	9	8	6	3	1	10	4
	Value	0.09	0.12	0.20	0.27	0.29	0.32	0.73	0.74	0.82	0.84

Figure 4 illustrates the decoding method, where Figure 4a displays the arrangement of the new sequence of elements to determine the positions of LoRaWAN gateways, and Figure 4b showcases the assignment of villages to these gateways. Commencing with Village 7 being assigned to the position of LoRaWAN gateway 1, Villages 7, 5, and 2 are allocated to this position as they meet the assignment criteria. Following that, Village 9, the second village in order, is assigned to the position of LoRaWAN gateway 2, along with Village 8, which also satisfies the assignment conditions. Similarly, Village 6, the third village in order, is assigned to the position of LoRaWAN gateway 3, along with Village 1. Lastly, Village 3 is assigned to the position of LoRaWAN gateway 4, together with Villages 10 and 4, as they fulfill the assignment conditions.

4.3.2. Updating Black Box Probability

Within our methodology, the tracks undergo continuous exploration within the Improvement box (IB), which encompasses advanced solution enhancement techniques that surpass simple local search. The IB consists of several methods, including DE-inspired move (DIM), random-transit (RT), best-transit (BT), and inter-transit (IT). The selection of the preferred method from the IB is determined using a roulette wheel selection approach, guided by Equation (11).

$$P_{bt} = \frac{FN_{bt-1} + (1 - F)A_{bt-1} + KI_{bt-1} + \rho |A_{bt-1} - A_{t-1}^{best}|}{\sum_{b=1}^B FN_{bt-1} + (1 - F)A_{bt-1} + KI_{bt-1} + \rho |A_{bt-1} - A_{t-1}^{best}|} \quad (11)$$

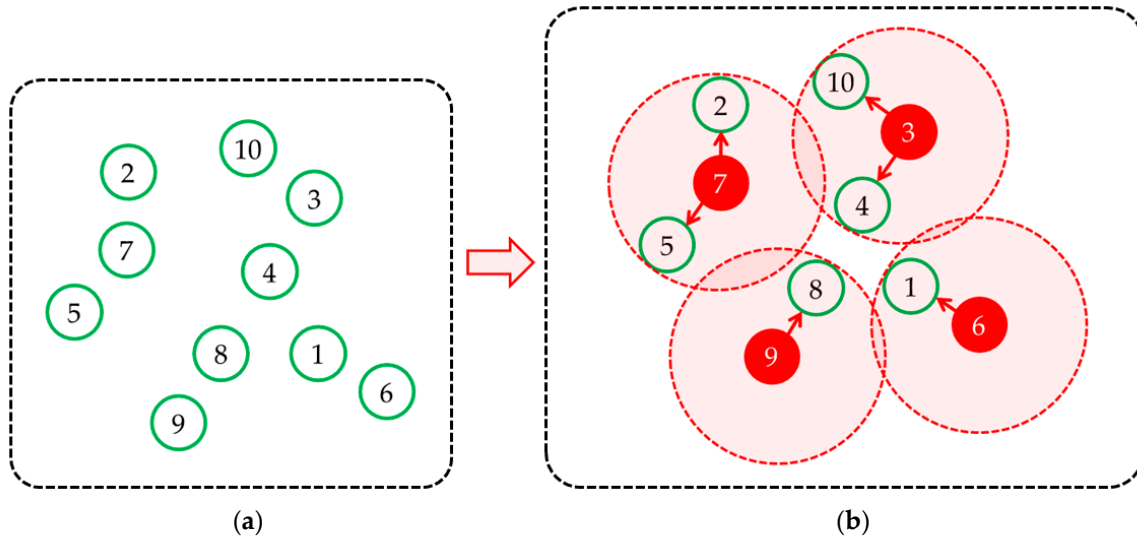


Figure 4. Decoding method. (a) The location of villages; (b) the assignment of villages to gateways.

In Equation (11), P_{bt} denotes the likelihood of choosing method b from the improvement box (IB) in iteration t . N_{bt-1} denotes the total number of tracks that have previously chosen method b . A_{bt-1} denotes the mean objective value across all tracks that have opted for method b in the previous iterations. A_{t-1}^{best} represents the objective value of the most optimal global solution identified before iteration t . I_{bt-1} denotes a reward value that increments by 1 when an intervention method from the bundle successfully identifies the solution with the highest level of optimality achieved in the previous iteration. In case the intervention method fails to identify such a solution, the reward value is set to 0. B denotes the total number of methods in the IB, while F and K represent scaling and parameter factors, respectively ($F = 0.5, K = 1$). Equation (11) guides the decision-making process for selecting the method from the IB in each iteration, considering four key factors that steer the solution towards promising search areas. These factors encompass the frequency at which tracks select the method, the average solution value of tracks that choose the method, the inclusion of current best solutions within the method, and the proximity of the average solution of tracks selecting the method to the solution of the best-performing method. It is important to note that if a method produces favorable solutions in previous iterations, its probability of being selected in the current iteration increases.

4.3.3. Improvement Box Operations

Within our methodology, we incorporate four improvement boxes, namely DE-inspired move, random transit, best transit, and inter-transit, as suggested by reputable sources [39–42]. These improvement boxes are executed using Equations (12)–(15).

$$\text{DE-inspired Move (DIM)} \quad Z_{ijt} = X_{rjt} + Q_{ij}(X_{rjt} - X_{njt}) \quad (12)$$

$$\text{Random-transit (RT)} \quad Z_{ijt} = \begin{cases} X_{ijt} & \text{if } Q_{ij} \leq CR \\ R_{ijt} & \text{otherwise} \end{cases} \quad (13)$$

$$\text{Best-transit (BT)} \quad Z_{ijt} = \begin{cases} X_{ijt} & \text{if } Q_{ij} \leq CR \\ B_{ijt} & \text{otherwise} \end{cases} \quad (14)$$

$$\text{Inter-transit (IT)} \quad Z_{ijt} = \begin{cases} X_{ijt} & \text{if } Q_{ij} \leq CR \\ X_{njt} & \text{otherwise} \end{cases} \quad (15)$$

In the above equations, Z_{ijt} represents the newly generated value at position j using the improvement boxes (IBs). During each iteration, X_{ijt} represents the value of element j in track i , where r and n denote different elements from the set of tracks (1 to E) that

are not equal to i . Q_{ij} is a randomly generated number for position j in track i , and R_{ijt} is a randomly generated number for element j in track i during iteration t , ranging from 0 to 1. The crossover rate (CR) is set at 0.8, following recommendations from reputable sources [42]. While our M-VaNSAS work builds upon the work in [39], we enhance it by incorporating an additional black box that employs DE mutation equations within the track improvement process, thereby introducing DE properties into the algorithm.

4.3.4. Track Update

During this step, we proceed to update specific heuristic information utilized in Equation (11), specifically addressing the variables outlined in Equation (16).

$$X_{ijt+1} = \begin{cases} Z_{ijt} & \text{if } f(Z_{ijt}) \geq f(X_{ijt}) \\ X_{ijt} & \text{otherwise} \end{cases} \quad (16)$$

As described in Equation (16), $f(Z_{ijt})$ represents the objective function value of Z_{ijt} , while $f(X_{ijt})$ represents the objective function value of X_{ijt} . To determine the track for the next iteration, we choose the one with the lower value between Z_{ijt} and X_{ijt} .

4.3.5. Repeat Sections 4.3.2–4.3.4

We continue the iterative process of executing Sections 4.3.2–4.3.4 until the specified termination criterion is satisfied, ensuring that this rigorous methodology is adhered to. Our primary objective is to methodically explore the solution space and identify the most optimal solutions for the specified problem. The M-VaNSAS algorithm (Algorithm 1), with its precisely defined steps and operators, presents a systematic and efficient approach to effectively addressing the challenges involved in optimizing gateway location selections within LoRaWANs. The pseudocode representation of the M-VaNSAS algorithm is presented below for reference.

The provided pseudocode presents a concise summary of the key procedures in the M-VaNSAS algorithm. It encompasses various steps, commencing with the generation of the initial population and continuing with iterative updates of the tracks until the predefined termination condition is met. Notably, it encompasses essential operations such as the initialization of initial tracks, the iterative adjustment of the probability associated with the black box, the execution of black box operations, and the subsequent updates of the tracks based on the values derived from the objective function. This pseudocode serves as a comprehensive guide to the implementation of the M-VaNSAS algorithm.

The gateway location selection problem falls within the category of NP-hard problems and is considered a generalized assignment problem. As the number of nodes increases, locating them within a limited time frame becomes impractical. To address this challenge, various metaheuristics, including genetic algorithms, ant colony optimization, simulated annealing, and M-VaNSAS, were devised to efficiently solve the problem within a constrained timeframe. M-VaNSAS, for instance, can yield feasible solutions with a time complexity of $O(T*PT*D)$, where T represents iterations, PT denotes the population of tracks, and D signifies dimensions.

Algorithm 1: M-VaNSAS

```

1   Section 4.3.1: Initial Population Generation
2   Initialize the population of tracks (PT)
3   Create an empty set for the initial tracks (IT)
4   Create an empty set for the best tracks (BT)
5   Create an empty set for the random tracks (RT)
6
7   for  $i = 1$  to NT do
8       Create a new track (T) of dimension  $1 \times D$ 
9       for  $j = 1$  to D do
10          Assign a random value to  $X_{ij1}$  using Equation (8)
11      end for
12      Add T to the initial tracks (IT)
13  end for
14
15  Generate random values for the best tracks (BT) using Equation (9)
16  Generate random values for the random tracks (RT) using Equation (10)
17
18  Section 4.3.2: Updating Black Box Probability (IB)
19  for  $t = 1$  to MaxIterations do
20      Calculate the probability  $P_{bt}$  for each black box using Equation (11)
21  end for
22
23  Section 4.3.3: Improvement Box Operations
24  for  $t = 1$  to MaxIterations do
25      for each track T in IT do
26          Select a black box operation (IB) based on the calculated probabilities
27          Perform the selected IB operation on T using Equations (12)–(15)
28      end for
29  end for
30
31  Section 4.3.4: Track Update
32  for each track T in IT do
33      Update track T by comparing the objective function values of the current track and the modified track using
34      Equation (16)
35  end for
36
37  Section 4.3.5: Repeat Sections 4.3.2–4.3.4
38  Repeat Sections 4.3.2–4.3.4 until the specified termination criterion is satisfied

```

4.4. Implementing Multi-Objective Optimization Methods

The segment dedicated to the implementation of multi-objective optimization methods comprises two key components: the Pareto front and TOPSIS. The Pareto front, recognized as the set of Pareto-optimal solutions, serves as a robust methodology for effectively managing conflicting objectives in decision-making. To assess the effectiveness of solutions within the Pareto front, we employ the technique for order of preference by similarity to the ideal solution (TOPSIS) for our analysis. TOPSIS aids in creating a normalized decision matrix, effectively transforming various attribute dimensions into non-dimensional attributes.

4.4.1. Pareto Front

The Pareto front, known as the Pareto-optimal solution set, serves as a powerful methodology for addressing the challenge of conflicting objectives in decision-making. In this study, we apply the Pareto front approach to the complex task of selecting optimal locations for multi-gateway deployment in large-scale LoRaWANs. Our objective is to

achieve a harmonious equilibrium between minimizing overall costs and maximizing bitrate, as shown in Equation (17).

$$f_{iq} = w^1 f_{iq}^1 + w^2 f_{iq}^2 \tag{17}$$

To formalize the problem, we utilize a general equation denoted as Equation (17), where the objective function f_{iq} represents target i during the q sub-calculation. Specifically, for our endeavor in multi-gateway deployment in LoRaWANs, we adopt Equation (18) as the objective function. The primary objective is to minimize total costs while concurrently maximizing the bitrate. Notably, the weights w^1 and w^2 correspond to the random allocation of significance to the first and second objectives, respectively, subject to the constraint that w^1 follows a uniform distribution $U(0, 1)$.

The objective functions f_{iq}^1 and f_{iq}^2 align with objectives z^1 and z^2 , respectively, illustrating the inherent conflict between these objectives. Equation (18) encapsulates the overarching objective, seeking to maximize Z . This equation skillfully balances the negative summation of costs (weighted by $-w^1$) against the positive summation of bitrate scores (weighted by w^2). By optimizing this equation, we can derive the Pareto-optimal values that strike a judicious compromise between cost reduction and achieving a high bitrate.

$$\text{Max } Z = \left(-w^1 \sum_{r=1}^R U_r Y_r \right) + \left(w^2 \sum_{v=1}^V \sum_{r=1}^R X_{rv} B_{rv} \right) \tag{18}$$

Within this context, the Pareto front assumes a crucial role in capturing the most favorable feasible solutions from a range of conflicting objectives. This approach enables the exploration of diverse deployment patterns in multi-gateway scenarios, taking into account cost optimization and the attainment of the highest possible bitrate. The objectives $f^1(y_r)$ and $f^2(y_r)$ represent the respective objective functions for targets 1 and 2 within the set R of viable options. Here, $y = (y_1, y_2, \dots, y_i)$ represents the collection of decision vectors, and $f^v(y) = (f^1(y), f^2(y), \dots, f^v(y))$ represents the collection of objective functions for vector y . It is important to note that the values of $f^v(y)$ hold greater significance than y' , and the condition $f^v(y) \leq f^v(y')$ must hold for $v = 1, 2, 3, \dots, V$.

4.4.2. Analyze Pareto Front Using TOPSIS

To evaluate the efficacy of the solutions within the Pareto front, we employ the technique for order of preference by similarity to the ideal solution (TOPSIS) [43] for our analysis. TOPSIS facilitates the development of a normalized decision matrix, which efficiently converts diverse attribute dimensions into non-dimensional attributes. This transformation, illustrated in Equations (19)–(25), establishes a standardized framework for comprehensive analysis and comparison of the solutions, ensuring a rigorous evaluation process.

$$r_{lv} = \frac{x_{lv}}{\sqrt{\sum_{l=1}^L (X_{lv})^2}} \tag{19}$$

$$U_{lv} = w_v r_{lv} \tag{20}$$

$$U_v^* = \{ \max_L U_{lv} \text{ if } v \in V; \min_L U_{lv} \text{ if } v \in V^* \} \tag{21}$$

$$U_v' = \{ \min_L U_{lv} \text{ if } v \in V; \max_L U_{lv} \text{ if } v \in V' \} \tag{22}$$

$$S_l^* = \sqrt{\sum_{v=1}^V (U_v^* - U_{lv})^2} \tag{23}$$

$$S_l' = \sqrt{\sum_{v=1}^V (U_v' - U_{lv})^2} \tag{24}$$

$$C_l^* = \frac{S_l'}{S_l^* + S_l'} \quad (25)$$

The TOPSIS method constructs a normalized decision matrix using Equations (19) and (20) to transform the attribute dimensions into non-dimensional attributes. Here, U_{lv} represents the non-dimensional attribute value for point l and objective v , while r_{lv} denotes the normalized value of the objective function. The predefined weights w_v determine the relative importance of each objective function. The positive ideal solution U_v^* and the negative ideal solution U_v' is represented by V^* and V' , respectively, which correspond to the sets of positive and negative objective functions. The separation measures S_l^* and S_l' are employed to quantify the distances between each alternative and the ideal solutions. These measures enable the calculation of proximity in relation to the ideal solution, denoted as C_l^* . The parameter set with the solution with a C_l^* value closest to 1 is considered the most favorable option, indicating its high degree of alignment with the ideal objectives.

5. Computational Results and Framework

This section presents a detailed analysis of the computational results and framework for optimizing the selection of multiple gateway locations in LoRaWANs. The experiments were conducted using the DE, GA, PSO, and M-VaNSAS algorithms, with the objective of minimizing system costs and maximizing bitrate. The obtained solutions were compared to evaluate the performance of each algorithm and provide valuable insights into their effectiveness. The proposed method was created using Python 3 and executed on Google Colab resources. The computational setup comprised an Intel(R) Xeon(R) CPU @ 2.20 GHz, accompanied by 12.7 GB of RAM and 107.7 GB of disk space.

5.1. The Solutions

The results revealed interesting findings and significant differences among the solutions generated using each algorithm. Firstly, the GA algorithm produced a set of solutions that achieved a range of cost and bitrate values. However, the trade-off between cost and bitrate was not optimal, as some solutions exhibited higher costs for relatively lower bitrates. This indicates that the GA algorithm struggled to effectively balance the two objectives. On the other hand, the DE algorithm performed slightly better than the GA algorithm in terms of achieving a more balanced trade-off between cost and bitrate. The solutions obtained with DE showed improvements in both cost reduction and bitrate maximization compared to the GA solutions. However, there were still instances where the achieved bitrates were not optimal, indicating room for further enhancement. The PSO algorithm exhibited promising results, with solutions that demonstrated a more favorable trade-off between cost and bitrate compared to both GA and DE. The solutions obtained from PSO achieved lower costs while maintaining higher bitrates, indicating a more efficient allocation of gateway locations. This suggests that the PSO algorithm was able to effectively explore the solution space and identify better solutions for analyzing the tradeoffs between system costs and bitrate maximization for the optimal selection of gateway locations in LoRaWANs.

Lastly, the M-VaNSAS algorithm, specifically designed for this problem, outperformed all other algorithms in terms of generating superior solutions. The solutions obtained from M-VaNSAS consistently achieved the best trade-off between system costs and bitrate maximization. This demonstrates the effectiveness of the proposed algorithm in generating optimized solutions for analyzing the tradeoffs between system costs and bitrate maximization for the optimal selection of gateway locations in LoRaWANs.

As seen in Figure 5, the solutions generated using GA, DE, PSO, and M-VaNSAS were thoroughly analyzed and compared based on their ability to optimize system costs and maximize bitrate. Figure 5a depicts the solutions obtained using GA, Figure 5b showcases the solutions of DE, Figure 5c displays the solutions generated using PSO, and Figure 5d illustrates the solutions obtained using M-VaNSAS. These figures provide a

visual representation of the solutions and allow for a comprehensive comparison of their quality and distribution.

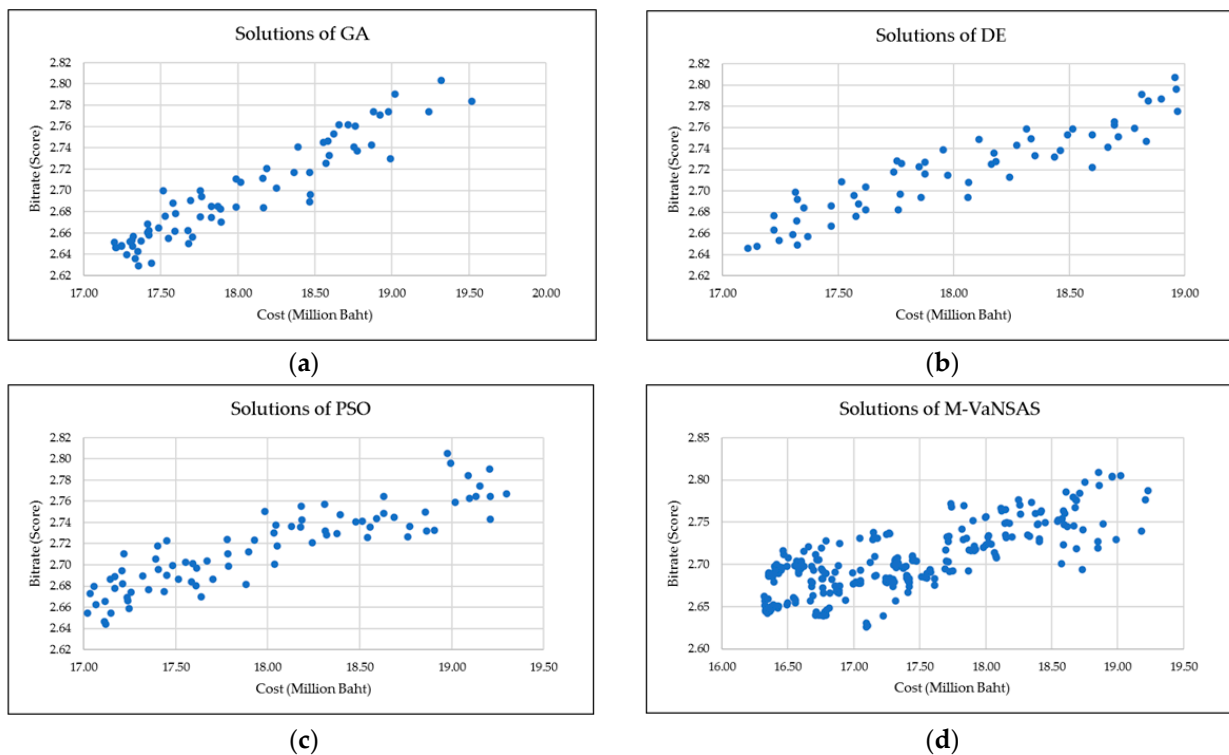


Figure 5. The solutions of GA, DE, PSO, and M-VaNSAS. (a) GA solutions; (b) DE solutions; (c) PSO solutions; (d) M-VaNSAS solutions.

In conclusion, the computational results and framework analysis highlight the strengths and weaknesses of the GA, DE, PSO, and M-VaNSAS algorithms for analyzing the trade-offs between system costs and bitrate maximization for the optimal selection of gateway locations in LoRaWANs. While each algorithm showed some level of effectiveness, the M-VaNSAS algorithm proved the most successful in achieving optimized solutions that minimize system costs while maximizing bitrate. These findings underscore the significance of developing specialized algorithms tailored to specific problem domains, as they can yield superior results compared to more general optimization algorithms.

5.2. The Pareto Front

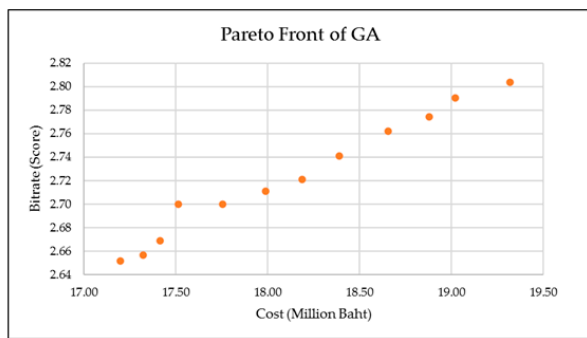
The Pareto front is a set of non-dominated solutions that represent the trade-off between multiple objectives in a multi-objective optimization problem. In this case, the objectives are the cost and bitrate values obtained using different algorithms, namely GA, DE, PSO, and M-VaNSAS. The Pareto fronts of GA, DE, PSO, and M-VaNSAS are shown in Table 7.

Table 7 presents the Pareto fronts of GA, DE, PSO, and M-VaNSAS. The GA Pareto front consists of 12 solutions with diverse cost and bitrate values, ranging from 17,199,066 to 19,318,163 and 2.652 to 2.803, respectively. These solutions offer a wide range of tradeoffs between cost and bitrate, showcasing the availability of multiple optimal choices. Similarly, the DE Pareto front comprises 12 solutions with cost values spanning from 17,110,691 to 18,958,206 and bitrate values from 2.646 to 2.807, indicating the algorithm’s ability to generate diverse optimal solutions across the cost-bitrate spectrum. The PSO Pareto front showcases 15 solutions with cost values ranging from 17,020,510 to 18,974,922 and bitrate values from 2.654 to 2.805, demonstrating the effectiveness of the PSO algorithm in exploring a broad range of cost and bitrate options. In contrast, the M-VaNSAS Pareto front

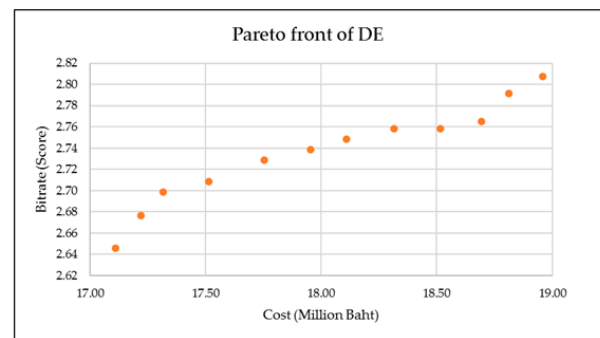
encompasses 14 solutions with cost values ranging from 16,319,264 to 18,854,515 and bitrate values from 2.662 to 2.809. Remarkably, the proposed M-VaNSAS method outperforms the other algorithms by providing solutions with lower costs and higher bitrates, emphasizing its superior performance. These Pareto fronts are visually represented with graphs in Figure 6.

Table 7. The Pareto fronts of GA, DE, PSO, and M-VaNSAS.

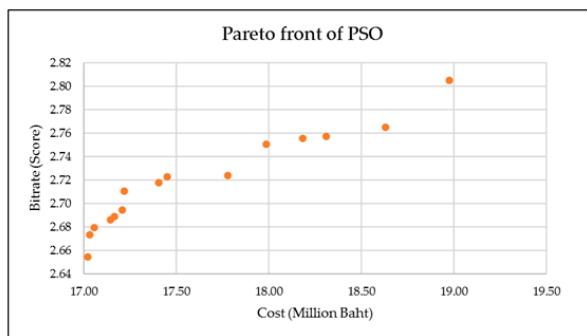
Solution	GA		DE		PSO		M-VaNSAS	
	Cost	Bitrate	Cost	Bitrate	Cost	Bitrate	Cost	Bitrate
1	17,199,066	2.652	17,110,691	2.646	17,020,510	2.654	16,319,264	2.662
2	17,321,326	2.657	17,221,326	2.677	17,033,243	2.673	16,353,115	2.690
3	17,414,942	2.669	17,315,962	2.699	17,055,891	2.680	16,401,418	2.698
4	17,514,961	2.700	17,514,961	2.709	17,145,411	2.686	16,412,228	2.700
5	17,754,869	2.700	17,754,964	2.729	17,167,132	2.689	16,464,458	2.716
6	17,988,424	2.711	17,954,977	2.739	17,208,063	2.694	16,655,943	2.721
7	18,188,724	2.721	18,110,352	2.748	17,218,460	2.710	16,790,745	2.728
8	18,388,784	2.741	18,314,881	2.759	17,403,181	2.718	17,043,297	2.731
9	18,655,918	2.762	18,514,935	2.759	17,451,993	2.723	17,148,339	2.738
10	18,878,803	2.774	18,694,467	2.765	17,779,202	2.724	17,733,606	2.772
11	19,020,279	2.791	18,812,312	2.791	17,984,142	2.750	18,246,791	2.776
12	19,318,163	2.803	18,958,206	2.807	18,183,687	2.755	18,610,309	2.786
13					18,310,776	2.757	18,750,295	2.797
14					18,630,940	2.765	18,854,515	2.809
15					18,974,922	2.805		



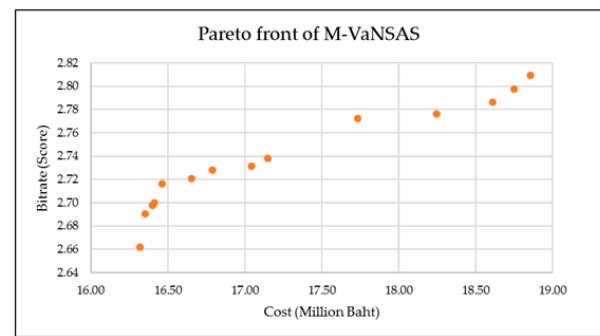
(a)



(b)



(c)



(d)

Figure 6. The Pareto fronts of GA, DE, PSO, and M-VaNSAS. (a) Pareto front of GA; (b) Pareto front of DE; (c) Pareto front of PSO; (d) Pareto front of M-VaNSAS.

Figure 6 depicts the Pareto fronts of GA, DE, PSO, and M-VaNSAS. Figure 6a showcases the Pareto front achieved using GA, Figure 6b illustrates the Pareto front of DE, Figure 6c displays the Pareto front obtained using PSO, and Figure 6d showcases the Pareto front

achieved using M-VaNSAS. Analyzing these Pareto fronts provides valuable insights into the performance of each algorithm in achieving an optimal balance between system costs and bitrate, enabling a comprehensive comparison of their capabilities. The visual representations in Figure 6 allow for a clear understanding of the tradeoffs and efficiency achieved using each algorithm. Furthermore, a direct comparison of the four Pareto fronts can be observed in Figure 7, providing a holistic view of their relative performance and effectiveness.

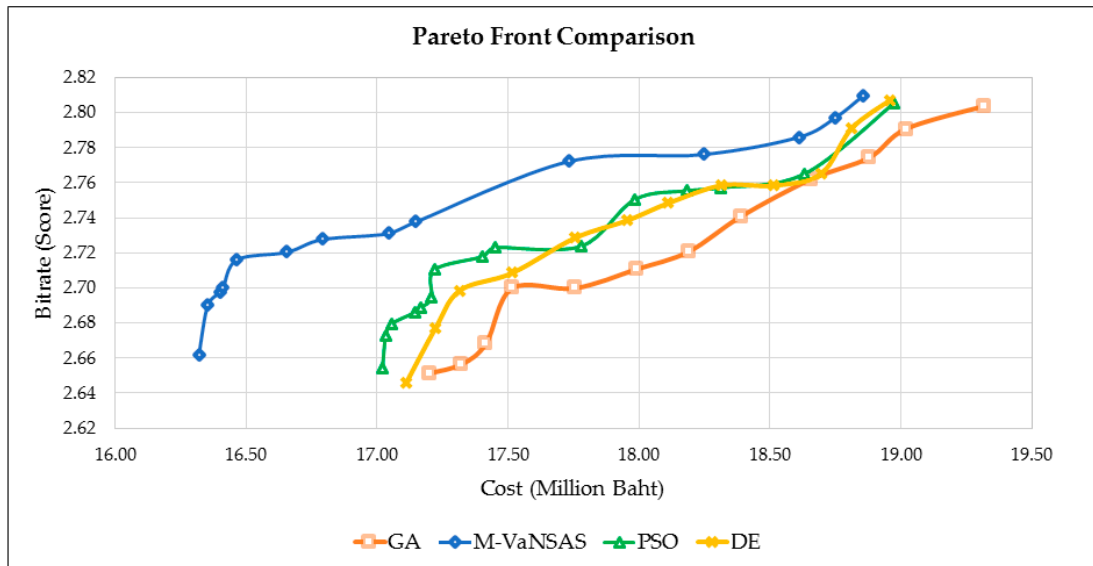


Figure 7. Pareto front comparison.

Figure 7 provides a comprehensive comparison of the proposed M-VaNSAS method with GA, DE, and PSO. The comparison reveals that M-VaNSAS exhibits superior performance in terms of both cost and bitrate. The Pareto front of M-VaNSAS showcases a narrower cost range and a wider bitrate range, indicating its ability to achieve more favorable tradeoffs between these objectives. These findings suggest that M-VaNSAS has the potential to outperform GA, DE, and PSO in addressing the optimization problem at hand.

In summary, the analysis of the Pareto fronts underscores the superiority of the proposed method, M-VaNSAS, over GA, DE, and PSO in terms of both cost and bitrate. The algorithm generates a diverse set of optimal solutions characterized by lower cost values and higher bitrate values, demonstrating its effectiveness in achieving superior tradeoffs. The outcomes emphasize the potential effectiveness of M-VaNSAS as a viable strategy in tackling comparable optimization challenges. This is due to the algorithm’s purposeful design for proficiently navigating solution spaces and identifying optimal gateway locations within a black box that integrates various methods, thereby imposing a considerable computational burden. Essential operations involve the execution of black box procedures and the adjustment of pathways based on objective function values. Our methodology involves continuous exploration of pathways within the improvement box, utilizing sophisticated solution enhancement techniques that surpass fundamental local searches.

5.3. TOPSIS Analysis

The Pareto front analysis of M-VaNSAS was further complemented by utilizing the TOPSIS method. TOPSIS involves assigning weights to different criteria to ascertain their relative significance in the decision-making process. The weights, represented by w^1 and w^2 in Table 8, correspond to the “Costs” and “Bitrate scores” criteria, respectively. The TOPSIS results of M-VaNSAS are presented in Table 8, providing valuable insights into the performance of the algorithm based on these weighted criteria.

Table 8. TOPSIS results of GA, DE, PSO, and M-VaNSAS.

Solution	w^1	w^2	GA		DE		PSO		M-VaNSAS	
			Cost	Bitrate	Cost	Bitrate	Cost	Bitrate	Cost	Bitrate
1	0.1	0.9	19,318,163	2.803	18,958,206	2.807	18,974,922	2.805	18,854,515	2.809
2	0.2	0.8	18,878,803	2.774	18,694,467	2.765	17,779,202	2.724	17,734,606	2.772
3	0.3	0.7	17,988,424	2.711	17,954,977	2.739	17,208,063	2.694	16,464,458	2.716
4	0.4	0.6	17,754,869	2.700	17,754,964	2.729	17,208,063	2.694	16,464,458	2.716
5	0.5	0.5	17,514,961	2.700	17,514,961	2.709	17,208,063	2.694	16,464,458	2.716
6	0.6	0.4	17,414,942	2.669	17,315,962	2.699	17,033,243	2.673	16,464,458	2.716
7	0.7	0.3	17,414,942	2.669	17,221,326	2.677	17,033,243	2.673	16,464,458	2.716
8	0.8	0.2	17,414,942	2.669	17,221,326	2.677	17,033,243	2.673	16,353,115	2.690
9	0.9	0.1	17,199,066	2.652	17,110,691	2.646	17,020,510	2.654	16,353,115	2.690

In Table 8, the TOPSIS results for GA, DE, PSO, and M-VaNSAS showcase the effectiveness of M-VaNSAS, as each of its solutions outperforms the other algorithms. Analyzing the TOPSIS results for M-VaNSAS reveals diverse weight distributions among different solutions, indicating varying importance assigned to the cost and bitrate criteria. For example, Solution 1 assigns a higher weight to the bitrate criterion ($w^2 = 0.9$) than the cost criterion ($w^1 = 0.1$). This results in a relatively higher cost (approximately THB 18,854,515) but an impressive bitrate score of 2.809. Similarly, Solution 2 emphasizes the bitrate criterion ($w^2 = 0.8$) while maintaining a lower cost (around THB 17,734,606) and a slightly reduced bitrate score of 2.772. Interestingly, Solutions 3, 4, 5, 6, and 7 exhibit a consistent weight distribution pattern with varying values, producing comparable cost values (approximately THB 16,464,458) and achieving a reliable bitrate score of 2.716. This suggests that these solutions strike a satisfactory balance between cost efficiency and data transmission quality. Conversely, Solutions 8 and 9 allocate a higher weight to the cost criterion ($w^1 = 0.8$), resulting in lower cost (around THB 16,353,115) at the expense of a slightly reduced bitrate score of 2.69. Figure 8 visually presents the TOPSIS results of M-VaNSAS, offering a graphical representation of each solution along with its corresponding characteristics.

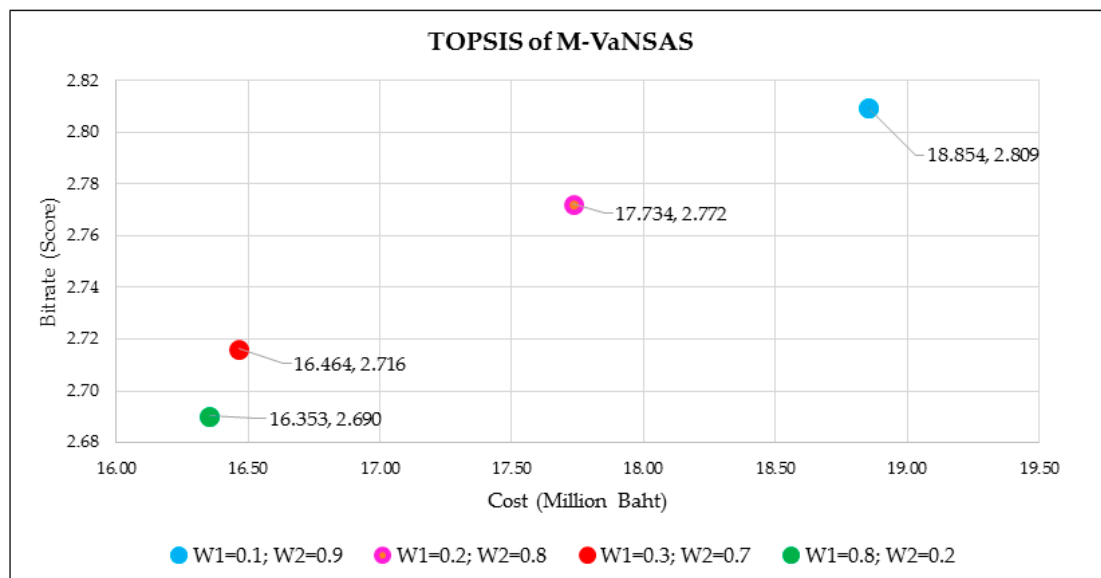


Figure 8. The TOPSIS of M-VaNSAS.

Figure 8 visually represents the TOPSIS analysis of M-VaNSAS, depicting the solutions grouped according to their performance. This detailed analysis provides a holistic assessment of the effectiveness of M-VaNSAS for analyzing the tradeoffs between system costs and bitrate maximization for the optimal selection of gateway locations in LoRaWANs and

offers valuable insights into the algorithm’s ability to optimize system costs and maximize bitrate. By understanding the grouping and characteristics of these solutions, decision-makers can make informed choices based on their specific priorities and requirements. The analysis provides valuable insights into the tradeoffs between cost and bitrate and enables stakeholders to select the most suitable solution group that aligns with their preferences.

5.4. Optimal Gateway Locations for LoRaWANs

This study conducted a comprehensive comparison of solutions, Pareto fronts, and TOPSIS analyses for DE, GA, PSO, and M-VaNSAS in the context of selecting multiple gateway locations in LoRaWANs. The results emphasized the optimal selection, showcasing a balanced tradeoff between cost and bitrate scores ($w^1 = 0.3, w^2 = 0.7$). To visually represent the chosen gateway locations, the study leveraged the advanced mapping capabilities of the QGIS (quantum geographic information system) program. This integration of analytical insights and geospatial visualization not only contributes to the advancement of IoT technologies but also facilitates the efficient deployment and management of IoT networks. Notably, the case study focused on a rural area, and results may vary in urban scenarios. In [23], it was recommended to evaluate LoRa network performance in diverse environments, including both rural and urban settings. By implementing this approach in the Ubon Ratchathani province, this study provides a comprehensive representation of optimal gateway locations, thereby enhancing connectivity and data transmission in LoRaWANs, as illustrated in Figure 9.

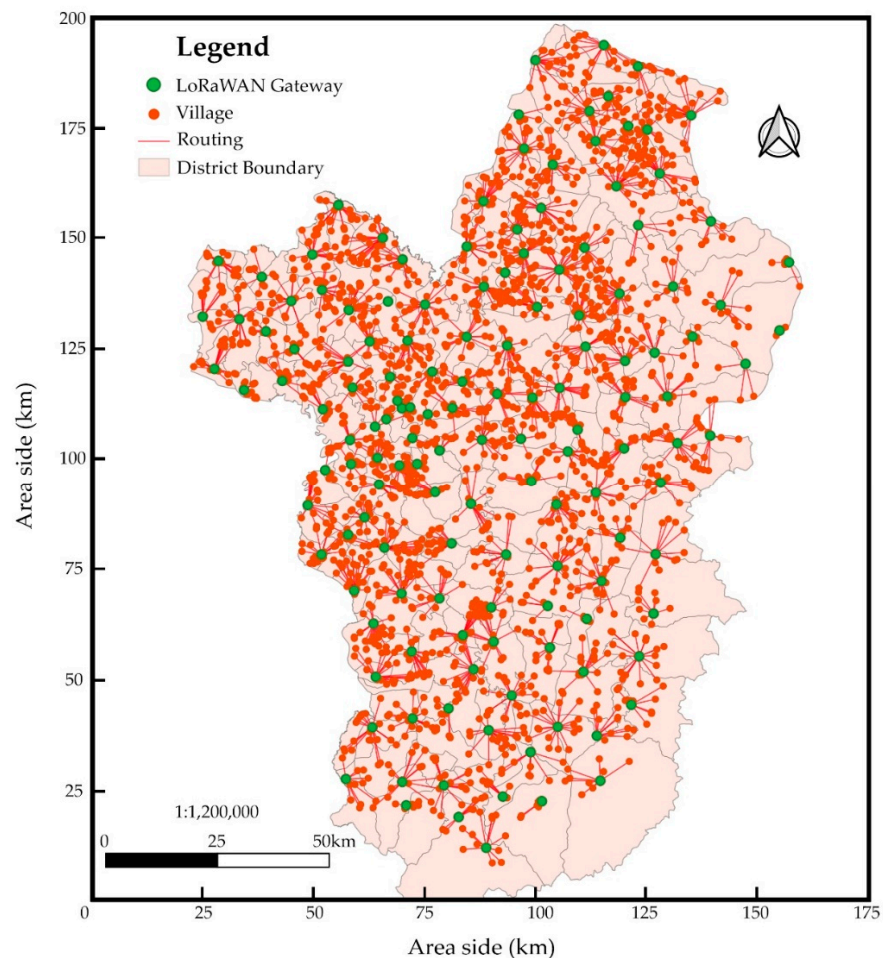


Figure 9. LoRaWAN infrastructure in Ubon Ratchathani province.

Figure 9 illustrates the results of a comprehensive analysis aimed at identifying optimal gateway locations for LoRaWANs in the Ubon Ratchathani province. The findings reveal

the positions of 144 gateways strategically placed to ensure efficient network infrastructure. These gateways are instrumental in providing reliable LoRaWAN signals to support smart farming initiatives, benefiting a substantial population of 295,942 households spread across 2199 villages. By utilizing the QGIS program's advanced mapping capabilities, the selected gateway locations are visualized, providing decision-makers and stakeholders valuable insights for infrastructure planning and optimization. This research contributes to the expansion of IoT technologies in agriculture, facilitating the integration of connected devices and enabling farmers to leverage the advantages of smart farming practices, thereby enhancing productivity and sustainability in the region.

6. Conclusions and Future Outlook

This study analyzed tradeoffs between system costs and bitrate maximization for the optimal selection of gateway locations in LoRaWANs. With the development of a mathematical model and the introduction of the M-VaNSAS algorithm, this research makes substantial contributions to the field. It provides valuable insights into the performance of various optimization algorithms and offers an efficient solution to address this complex problem. The computational findings and framework analysis provide evidence of the efficacy of the proposed M-VaNSAS algorithm in comparison to widely used optimization algorithms such as GA, DE, and PSO. The solutions generated using M-VaNSAS consistently outperformed the other algorithms in terms of system costs and bitrate, indicating its ability to strike a favorable balance between these two critical factors. Pareto front analysis further revealed the tradeoffs between system costs and bitrate, with M-VaNSAS offering a wider range of optimal solutions along the Pareto front. Additionally, the TOPSIS analysis provided a comprehensive evaluation of the M-VaNSAS algorithm by assigning weights to different criteria. The results demonstrate its consistent ability to optimize system costs and maximize bitrate, further reinforcing its effectiveness in real-world scenarios. These findings underscore the superiority of M-VaNSAS and its potential for practical implementation in optimizing multiple gateway location selection in LoRaWANs.

In conclusion, this research presented the M-VaNSAS algorithm and conducted a comprehensive comparative analysis. The results highlight its superiority in achieving cost-effective and high-performing LoRaWANs. The insights gained from this study have significant implications for the deployment and operation of IoT applications in various environments. Ultimately, these findings contribute to the advancement of research in network planning and pave the way for improved connectivity and efficient resource utilization in the context of smart city development.

Our research centered on optimizing the positioning of LoRaWAN gateways, utilizing data from a province in Thailand. It is important to note that the limitations of our study pertain specifically to rural areas in Thailand. Future research endeavors should extend their focus to evaluating LoRa network performance in diverse environments, encompassing both rural and urban settings. High mountain areas present challenges to LoRa signal propagation, affecting the performance and efficiency of LoRaWANs. Overcoming these challenges would contribute to advancing the optimization of selecting multiple gateway locations and supporting the overall growth of IoT technologies.

Author Contributions: Conceptualization, C.S. and C.K.; methodology, C.S. and C.K.; software, C.K.; validation, C.K.; investigation, C.S.; writing—original draft preparation, C.K.; writing—review and editing, C.S. and C.K.; visualization, C.K.; supervision, C.S. All authors have read and agreed to the published version of the manuscript.

Funding: This research received no external funding.

Data Availability Statement: The use of the VaNSAS algorithm with data can be observed on <https://github.com/GitChut/VaNSAS-LoRaWAN> (accessed on 25 November 2023).

Conflicts of Interest: The authors declare no conflicts of interest.

References

1. Food Security Information Network. *World Food Programme Global Report on Food Crises 2022*; Food Security Information Network: Bogotá, Colombia, 2022; 277p.
2. Atzori, L.; Iera, A.; Morabito, G. The Internet of Things: A survey. *Comput. Netw.* **2010**, *54*, 2787–2805. [[CrossRef](#)]
3. Moysiadis, V.; Sarigiannidis, P.; Vitsas, V.; Khelifi, A. Smart Farming in Europe. *Comput. Sci. Rev.* **2021**, *39*, 100345. [[CrossRef](#)]
4. Akpakwu, G.A.; Silva, B.J.; Hancke, G.P.; Abu-Mahfouz, A.M. A Survey on 5G Networks for the Internet of Things: Communication Technologies and Challenges. *IEEE Access* **2017**, *6*, 3619–3647. [[CrossRef](#)]
5. Ahmadi, H.; Arji, G.; Shahmoradi, L.; Safdari, R.; Nilashi, M.; Alizadeh, M. *The Application of Internet of Things in Healthcare: A Systematic Literature Review and Classification*; Springer: Berlin/Heidelberg, Germany, 2019; Volume 18.
6. Faheem, M.; Shah, S.B.H.; Butt, R.A.; Raza, B.; Anwar, M.; Ashraf, M.W.; Ngadi, M.A.; Gungor, V.C. Smart grid communication and information technologies in the perspective of Industry 4.0: Opportunities and challenges. *Comput. Sci. Rev.* **2018**, *30*, 1–30. [[CrossRef](#)]
7. Pasolini, G.; Buratti, C.; Feltrin, L.; Zabini, F.; de Castro, C.; Verdone, R.; Andrisano, O. Smart city pilot projects using LoRa and IEEE802.15.4 technologies. *Sensors* **2018**, *18*, 1118. [[CrossRef](#)] [[PubMed](#)]
8. Miles, B.; Bourennane, E.B.; Boucherkha, S.; Chikhi, S. A study of LoRaWAN protocol performance for IoT applications in smart agriculture. *Comput. Commun.* **2020**, *164*, 148–157. [[CrossRef](#)]
9. Hassan, W.; Føre, M.; Ulvund, J.B.; Alfredsen, J.A. Internet of Fish: Integration of acoustic telemetry with LPWAN for efficient real-time monitoring of fish in marine farms. *Comput. Electron. Agric.* **2019**, *163*, 104850. [[CrossRef](#)]
10. Triantafyllou, A.; Sarigiannidis, P.; Lagkas, T.; Moscholios, I.D.; Sarigiannidis, A. Leveraging fairness in LoRaWAN: A novel scheduling scheme for collision avoidance. *Comput. Netw.* **2021**, *186*, 107735. [[CrossRef](#)]
11. Semtech Corporation. *LoRa and LoRaWAN: A Technical Overview*; Semtech Corporation: Camarillo, CA, USA, 2019.
12. Adelantado, F.; Vilajosana, X.; Tuset-Peiro, P.; Martinez, B.; Melia-Segui, J.; Watteyne, T. Understanding the Limits of LoRaWAN. *IEEE Commun. Mag.* **2017**, *55*, 34–40. [[CrossRef](#)]
13. Mekki, K.; Bajic, E.; Chaxel, F.; Meyer, F. A comparative study of LPWAN technologies for large-scale IoT deployment. *ICT Express* **2019**, *5*, 1–7. [[CrossRef](#)]
14. Raza, U.; Kulkarni, P.; Sooriyabandara, M. Low Power Wide Area Networks: An Overview. *IEEE Commun. Surv. Tutor.* **2017**, *19*, 855–873. [[CrossRef](#)]
15. Truong, V.T.; Nayyar, A.; Lone, S.A. System performance of wireless sensor network using LoRa-Zigbee hybrid communication. *Comput. Mater. Contin.* **2021**, *68*, 1615–1635. [[CrossRef](#)]
16. Vejlggaard, B.; Lauridsen, M.; Nguyen, H.; Kovacs, I.Z.; Mogensen, P.; Sørensen, M. Interference impact on coverage and capacity for low power wide area IoT networks. In Proceedings of the 2017 IEEE Wireless Communications and Networking Conference (WCNC), San Francisco, CA, USA, 19–22 March 2017.
17. Fragkopoulos, M.; Panagiotakis, S.; Kostakis, M.; Markakis, E.K.; Astyrakakis, N.; Malamos, A. Experimental Assessment of Common Crucial Factors That Affect LoRaWAN Performance on Suburban and Rural Area Deployments. *Sensors* **2023**, *23*, 1316. [[CrossRef](#)] [[PubMed](#)]
18. Loh, F.; Mehling, N.; Geißler, S.; Hoßfeld, T. Efficient graph-based gateway placement for large-scale LoRaWAN deployments. *Comput. Commun.* **2023**, *204*, 11–23. [[CrossRef](#)]
19. Trendov, S.; Gering, M.; Siemens, E. Impact of LoRaWAN Transceiver on End Device Battery Lifetime. In Proceedings of the 2023 30th International Conference on Systems, Signals and Image Processing (IWSSIP), Ohrid, North Macedonia, 27–29 June 2023; pp. 1–5.
20. Correia, F.P.; Ruthielle, S.; Braga, F.; De Carvalho, S.; De Alencar, M.S.; Day, K.; Assis, R.; Bacurau, R.M. LoRaWAN Gateway Placement in Smart Agriculture : An Analysis of Clustering Algorithms and Performance Metrics. *Energies* **2023**, *16*, 2356. [[CrossRef](#)]
21. Frankiewicz, A.; Glos, A.; Grochla, K.; Łaskarzewski, Z.; Mischczak, J.; Polys, K.; Sadowski, P.; Strzoda, A. LP WAN Gateway Location Selection Using Modified K-Dominating Set Algorithm. In *Modelling, Analysis, and Simulation of Computer and Telecommunication Systems, Proceedings of the 28th International Symposium, MASCOTS 2020, Nice, France, 17–19 November 2020*; Springer International Publishing: Cham, Switzerland, 2021; Volume 12527 LNCS, pp. 209–223.
22. Kaewta, C.; Savithi, C.; Naenudorn, E. An optimization of multiple gateway location selection in long range wide area network networks. *Indones. J. Electr. Eng. Comput. Sci.* **2023**, *30*, 1011–1020. [[CrossRef](#)]
23. Griva, A.I.; Boursianis, A.D.; Wan, S.; Sarigiannidis, P.; Psannis, K.E.; Karagiannidis, G.; Goudos, S.K. LoRa-Based IoT Network Assessment in Rural and Urban Scenarios. *Sensors* **2023**, *23*, 1695. [[CrossRef](#)]
24. da Silva, C.N.; de Abreu, P.F.F.; da Silveira, J.D.F.; da Silveira, J.D. V Estimating the number of gateways through placement strategies in a LoRaWAN network. In Proceedings of the 2022 XII Brazilian Symposium on Computing Systems Engineering (SBESC), Fortaleza, Brazil, 21–24 November 2022; pp. 1–6.
25. Matni, N.; Moraes, J.; Oliveira, H.; Rosário, D.; Cerqueira, E. Lorawan gateway placement model for dynamic internet of things scenarios. *Sensors* **2020**, *20*, 4336. [[CrossRef](#)]
26. Tian, H.; Weitnauer, M.A.; Nyengele, G. Optimized gateway placement for interference cancellation in transmit-only LPWA networks. *Sensors* **2018**, *18*, 3884. [[CrossRef](#)]

27. Gravalos, I.; Makris, P.; Christodouloupoulos, K.; Varvarigos, E.A. Efficient Gateways Placement for Internet of Things with QoS Constraints. In Proceedings of the 2016 IEEE Global Communications Conference (GLOBECOM), Washington, DC, USA, 4–8 December 2016; pp. 1–6.
28. Askhedkar, A.R.; Chaudhari, B.S. Multi-Armed Bandit Algorithm Policy for LoRa Network Performance Enhancement. *J. Sens. Actuator Netw.* **2023**, *12*, 38. [[CrossRef](#)]
29. Bor, M.; Roedig, U.; Voigt, T.; Alonso, J.M. Do LoRa low-power wide-area networks scale? In Proceedings of the 19th ACM International Conference on Modeling, Analysis and Simulation of Wireless and Mobile Systems, New York, NY, USA, 13–17 November 2016; pp. 59–67.
30. Pasetti, M.; Sisinni, E.; Ferrari, P.; Rinaldi, S.; Depari, A.; Bellagente, P.; Giustina, D. Della; Flammini, A. Evaluation of the use of class B LoraWAN for the coordination of distributed interface protection systems in smart grids. *J. Sens. Actuator Netw.* **2020**, *9*, 13. [[CrossRef](#)]
31. Bidell, A.; Liu, Y.; Liang, H. LoRa Gateway Placement Optimization Based on a Data-Driven Low Height Path Loss Model. In Proceedings of the 2021 IEEE Canadian Conference on Electrical and Computer Engineering (CCECE), London, ON, Canada, 12–17 September 2021; pp. 1–6.
32. Al Mojamed, M. A Duty Cycle-Based Gateway Selection Algorithm for LoRaWAN Downlink Communication. *Comput. Syst. Sci. Eng.* **2023**, *45*, 2953–2970. [[CrossRef](#)]
33. Wu, W.; Wang, H.; Cheng, Z. ReLoRaWAN: Reliable data delivery in LoRaWAN networks with multiple gateways. *Ad Hoc Netw.* **2023**, *147*, 103203. [[CrossRef](#)]
34. LoRa™ Alliance. *LoRaWAN™ Regional Parameters v1.1rA*, LoRaWAN™ 1.1 Specification. 2017; 56p. Available online: <https://resources.lora-alliance.org/technical-specifications/lorawan-specification-v1-1> (accessed on 28 November 2023).
35. Nicolas, D.; Dominique, R.; Ahmed, S.; Olivier, H.; Gabor, P.; Guillaume, R. LoRa Device Developer Guide, Orange Connected Objects and Partnership Tech Doc. Available online: <https://developer.orange.com/od-uploads/LoRa-Device-Developer-Guide-Orange.pdf> (accessed on 12 August 2023).
36. Ramli, M.R.; Daely, P.T.; Kim, D.S.; Lee, J.M. IoT-based adaptive network mechanism for reliable smart farm system. *Comput. Electron. Agric.* **2020**, *170*, 105287. [[CrossRef](#)]
37. Haversine Formula. Wikipedia. Available online: https://en.wikipedia.org/wiki/Haversine_formula (accessed on 20 November 2023).
38. Jirasirilerd, G.; Pitakaso, R.; Sethanan, K.; Kaewman, S.; Sirirak, W.; Kosacka-Olejnik, M. Simple assembly line balancing problem type 2 by variable neighborhood strategy adaptive search: A case study garment industry. *J. Open Innov. Technol. Mark. Complex.* **2020**, *6*, 21. [[CrossRef](#)]
39. Sangkaphet, P.; Pitakaso, R.; Sethanan, K.; Nanthasamroeng, N.; Pranet, K.; Khonjun, S.; Srichok, T.; Kaewman, S.; Kaewta, C. A Multiobjective Variable Neighborhood Strategy Adaptive Search to Optimize the Dynamic EMS Location–Allocation Problem. *Computation* **2022**, *10*, 103. [[CrossRef](#)]
40. Pitakaso, R.; Nanthasamroeng, N.; Srichok, T.; Khonjun, S.; Weerayuth, N.; Kotmongkol, T.; Pornprasert, P.; Pranet, K. A Novel Artificial Multiple Intelligence System (AMIS) for Agricultural Product Transborder Logistics Network Design in the Greater Mekong Subregion (GMS). *Computation* **2022**, *10*, 126. [[CrossRef](#)]
41. Lipowski, A.; Lipowska, D. Roulette-wheel selection via stochastic acceptance. *Phys. A Stat. Mech. Its Appl.* **2012**, *391*, 2193–2196. [[CrossRef](#)]
42. Pitakaso, R.; Nanthasamroeng, N.; Dinkoksung, S.; Chindaprasert, K.; Sirirak, W.; Srichok, T.; Khonjun, S.; Sirisan, S.; Jirasirilerd, G.; Chomchalao, C. Solving the Optimal Selection of Wellness Tourist Attractions and Destinations in the GMS Using the AMIS Algorithm. *Computation* **2022**, *10*, 165. [[CrossRef](#)]
43. Hwang, C.-L.; Yoon, K. Methods for Multiple Attribute Decision Making. In *Multiple Attribute Decision Making*; Springer: Berlin/Heidelberg, Germany, 1981; pp. 58–191.

Disclaimer/Publisher’s Note: The statements, opinions and data contained in all publications are solely those of the individual author(s) and contributor(s) and not of MDPI and/or the editor(s). MDPI and/or the editor(s) disclaim responsibility for any injury to people or property resulting from any ideas, methods, instructions or products referred to in the content.